Vol. 41 (2010) ACTA PHYSICA POLONICA B No 2

IMAGING THE DECAY OF ^{8}He*

S. Mianowski, H. Czyrkowski, R. Dąbrowski, W. Dominik
Z. Janas, K. Miernik, M. Pfützner

Faculty of Physics, University of Warsaw
Hoża 69, 00-681 Warsaw, Poland

A.S. Fomichev, M.S. Golovkov, L.V. Grigorenko, S.A. Krupko
S.I. Sidorchuk, R.S. Slepnev, S.V. Stepantsov G.M. Ter-Akopian

Joint Institute for Nuclear Research
141980 Dubna, Moscow Region, Russia

(Received January 5, 2010)

The feasibility of the β decay study of ^{8}He with the use of a time projection chamber has been investigated. It is shown that β-delayed neutron emission branches of ^{8}He can be identified by registration of tracks of the recoiling ^{7}Li nuclei. Evidence for neutron emission from a highly excited ^{8}Li state was obtained. New possibilities to study β-decay of ^{8}He into the $\alpha+t+n$ continuum are demonstrated by showing that the full kinematics of such events can be reconstructed. Observed correlations will provide new insight into the mechanism of this decay process. Planned developments of the detection setup are discussed.

PACS numbers: 29.40.Cs, 29.30.Ep

1. Introduction

The nucleus of ^{8}He is characterized by the largest neutron-to-proton ratio among all known particle-stable nuclei. Various properties of this isotope have been already studied, recent highlights being the first nuclear charge radius determination [1] and precise mass measurement [2].

Beta decay of ^{8}He has been investigated in Refs. [3–5], where β-delayed γ-ray, neutron and triton spectra were measured. Comprehensive theoretical study of ^{8}He β-decay was presented in Ref. [6]. Fig. 1 shows the decay scheme of ^{8}He resulting from these studies. Beta decay of ^{8}He proceeds via Gamow–Teller transitions to 1^+ excited states of ^{8}Li. The most intense β-transition

* Presented at the XXXI Mazurian Lakes Conference on Physics, Piaski, Poland, August 30–September 6, 2009.

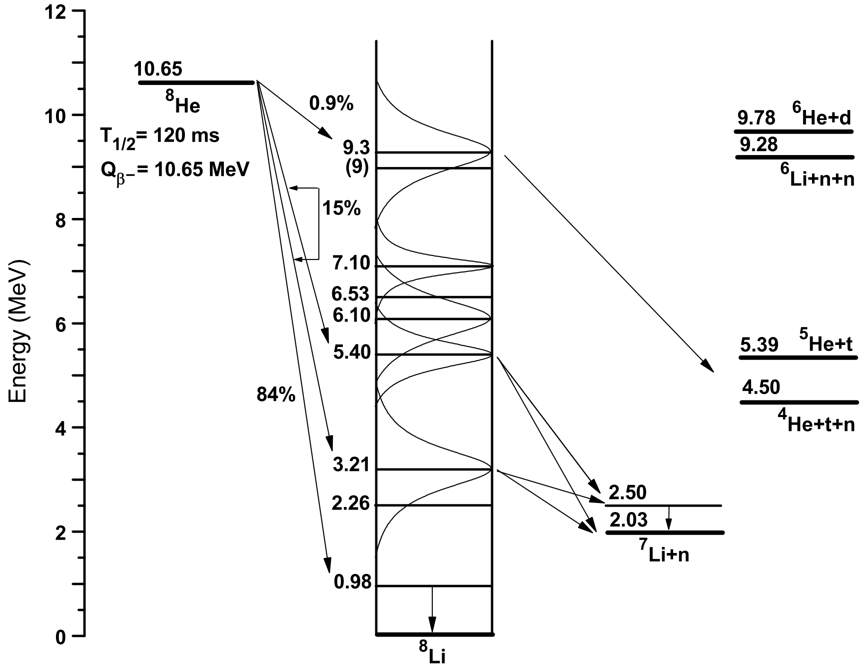

Fig. 1. Decay scheme of ^{8}He. The widths of ^{8}Li states are represented by the Lorentzian distributions.

feeds particle-bound ^{8}Li 1^+ state at the excitation energy of 0.98 MeV. About 15% of the ^{8}He decays feed (in unknown proportions) broad 1^+ resonances in ^{8}Li at 3.21 and 5.40 MeV. These states decay by neutron emission to the ground- and first excited state of ^{7}Li. Close to 1% of the ^{8}He decays feed a resonance at 9.3 MeV, which breaks up into an α particle, a triton and a neutron. The B(GT) value for this transitions was estimated to be 5.2, which is one of the highest values ever observed. It should still be considered as a lower limit since other possible decay channels of the 9.3 MeV resonance — neutron emission to ^{7}Li states, deuteron emission or two neutron decay — were not identified so far. Such a high B(GT) value was interpreted as an evidence for a transition between halo-analog states characterized by large overlap of their wave functions [7].

In this contribution we present first results of our attempt to study the decay of ^{8}He with the use of a new version of time projection chamber with optical readout (OTPC) [8, 9]. This device, originally developed to study two proton radioactivity [10], allows a full kinematic reconstruction of decay events and offers new possibilities to study the decay properties of ^{8}He.

2. Experimental technique

2.1. Production and identification of ^{8}He

The experiment was performed at the FLNR in Dubna, Russia. The ^{8}He ions were produced in fragmentation reaction of a 33 MeV/nucleon ^{11}B beam from the U-400 cyclotron impinging on a 275 mg/cm^2 thick carbon target. The ^{8}He ions with energy 23 AMeV were separated from unwanted reaction products by the ACCULINNA [11] fragment separator and transferred to the final focal plane where the OTPC detector was installed. Selected reaction products were identified in-flight by the time-of-flight (TOF) and the energy loss (ΔE) measurement with the use of the two 0.54 mm thick plastic scintillators installed on a 8.4 m base. The ^{8}He ions entered the active volume of the OTPC through a thin window in the side wall of the chamber, parallel to the electrodes plane, about 7.5 cm above the amplification section (see Sec. 2.2). Their energy (range) was adjusted by using an aluminium degrader placed in front of the entrance window.

2.2. Optical Time Projection Chamber

The OTPC detector [8, 9] consists of a set of parallel 20 cm × 20 cm electrodes forming several electric field regions (see Fig. 2). Active volume of the detector has a length of 30 cm. A whole volume of the OTPC was filled with a gas mixture of 95% of He and 5% of N_2 at atmospheric pressure. Such gas mixture was chosen to have long enough tracks of low energy decay products of ^{8}He.

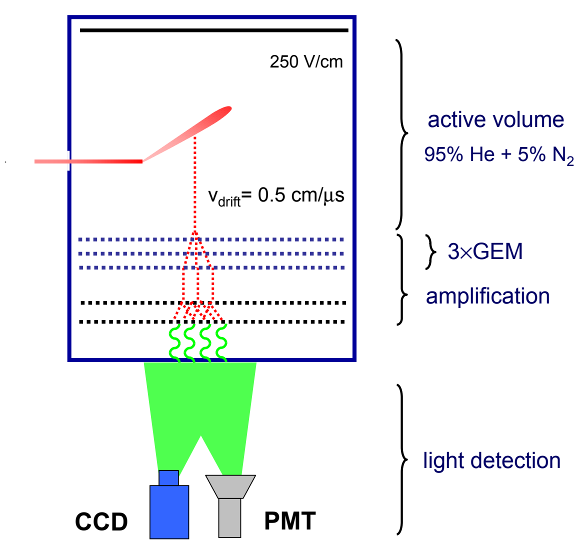

Fig. 2. Schematic view of the Optical Time Projection Chamber.

Incoming ions as well as their charged decay products produced ionization electrons along their trajectories in the gas filling the chamber. These primary ionization electrons were transported with a drift velocity of $v_{\rm d} = 0.5$ cm/μs towards two stage charge amplification structures. First of them was formed by three gas electron multiplier (GEM) foils [12], second one by two closely spaced wire-mesh electrodes. At the final amplification stage ultraviolet and visible photons were emitted. A visible part of this light spectrum was recorded by a 2/3" 1M pixel CCD camera with light amplification and a 5" photomultiplier (PMT). The data acquisition was triggered by a coincidence of a TOF signal and a PMT signal which provided a signature of a ^{8}He ion entering the OTPC detector. At the arrival of the trigger signal, the beam from the separator was switched off and the exposure of the camera was initiated for a period of 1–1.2 s. At the end of this time interval the camera image, the digitized PMT signal, and the ΔE–TOF information of the triggering ion were saved on a hard disk.

While the camera registered the projection of a particle's track on the electrode plane, the shape (width) of the time distribution of a PMT signal provided information on the track's projection in the direction normal to the image plane ($\Delta L_z = v_{\rm d}\Delta t$). The combination of information contained in the camera image and in the recorded drift time profile allows a complete reconstruction of particle's momentum. In the applied procedure the energy and particle emission angle were determined by fitting the projected theoretical ionization density distributions simulated by using SRIM [13] code to the light intensity distributions measured by the CCD and PMT. Fit parameters were a normalization factor, the energy and the emission angle. The experimentally determined response function of the OTPC detector was taken into account when comparing the calculated and measured profiles.

3. Results

3.1. Beta-delayed neutron decay of ^{8}He

Although the OTPC detector is not sensitive to neutrons, neutron emission from the excited ^{8}Li states could be observed by detection of ^{7}Li recoils if the track of the recoiling ion had the length sufficient for the reconstruction procedure to be applied. For the OTPC setup used in the ^{8}He study the minimal track length amounted to $\sim$ 10 mm which corresponds to the minimal ^{7}Li recoil energy of $\sim$ 0.2 MeV and minimal measurable neutron energy of about 1.4 MeV. Fig. 3 shows an example event of a β-delayed neutron decay of ^{8}He which occurred 252 ms after ion arrival. Tracks of the implanted ^{8}He ion (entering from the left side) and recoiling ^{7}Li are visible in the CCD camera image collected for 1.2 s. Shapes of the light intensity profiles recorded by the camera and the PMT are very well described by a calculated ionization density distribution of a ^{7}Li ion with an energy of

800 keV emitted at the polar angle (measured with respect to the electric field direction) of $\theta = 105°$. This recoil energy corresponds to the Q-value of 6.4 MeV. Assuming the neutron transition to the ground-state (first excited state) of ^{7}Li, the excitation energy of the initial ^{8}Li state amounts to 8.43 MeV (8.9 MeV). This value indicates that most probably neutron emission contributes to the decay of the halo-analog state in ^{8}Li. The branching ratio for this decay channel is to be determined.

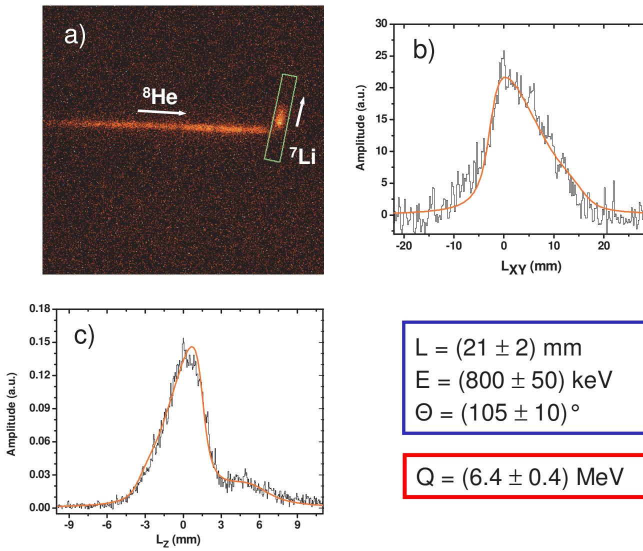

Fig. 3. An example event of a β-delayed neutron decay of ^{8}He. Panel (a) shows the image recorded by the CCD camera during a 1.2 s exposure. Plot (b) shows the distribution of the intensity of the CCD signal integrated along the ^{7}Li track. Plot (c) shows the time variation of the light intensity recorded by the PMT for the decay event. Time intervals were converted into the distance by using the drift velocity. Solid lines in plots (b) and (c) show the results of the fitting procedure. The obtained range, energy and emission angle of ^{7}Li recoil as well as the deduced decay Q-value are given in the bottom right part of the figure.

3.2. Beta-delayed triton decay of ^{8}He

Fig. 4 shows an example event of the β-decay of ^{8}He into the $\alpha + t + n$ continuum. Track of an implanted ^{8}He ion and tracks of two charged particles (α and t) emitted simultaneously (see Fig. 4 plot (b)) 90 ms after ion arrival are visible in the CCD camera image. A 1.5 cm displacement of the decay vertex with respect of the ^{8}He ion stopping position is consistent with the possible ion drift with the gas flow in the chamber. Solid line in Fig. 4 plot (b) shows that the shape of the light intensity recorded by the PMT

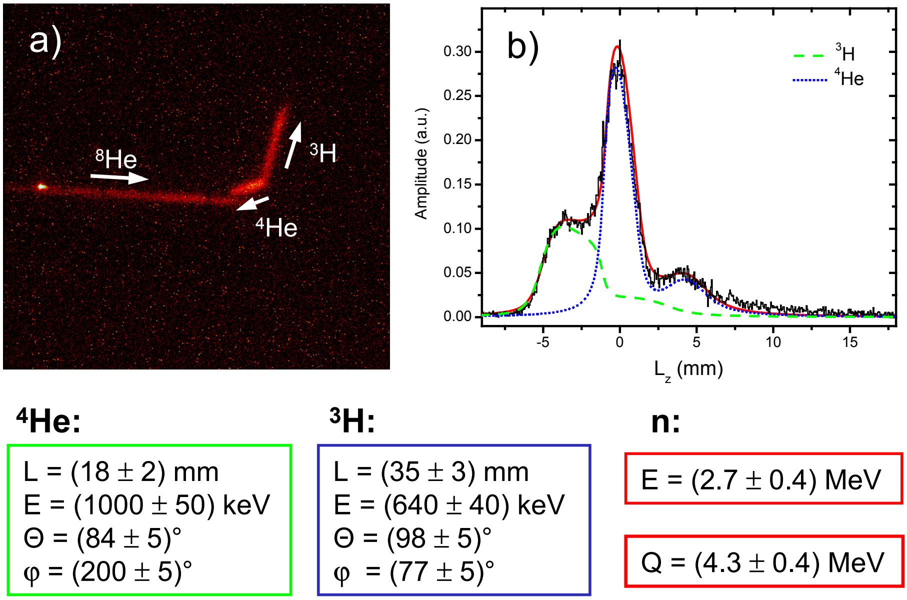

Fig. 4. An example event of a β-delayed triton decay of ^{8}He. Panel (a) shows an image recorded by the CCD camera during a 1 s exposure. Plot (b) shows the time variation of the light intensity recorded by the PMT for the decay event. Time intervals were converted into the distance by using the drift velocity. Dotted and dashed lines in plot (b) show the decomposition of the PMT signal into the parts corresponding to the α particle and triton detection, respectively. The resulting ranges, energies and emission angles of α particle and triton as well as reconstructed energy of the neutron are given in the bottom of the figure.

is very well described by the calculated ionization density distribution of an α particle with the energy of 1000 keV emitted at the polar angle $\theta = 84°$ and a triton with the energy of 640 keV emitted at the angle $\theta = 98°$. The energy of the neutron emitted in the decay was determined by momentum conservation requirement and this procedure yielded the value of 2.7 MeV. Thus, the total energy released in the decay event shown in Fig. 4 amounts to 4.3 MeV and gives 8.8 MeV as an excitation energy of the initial ^{8}Li state.

3.3. Beta decay of ^{8}Li

The 84% transitions in the β decay of ^{8}He proceed to the 1^+ state of ^{8}Li at 0.98 MeV which deexcites to the ground-state by a γ-ray emission. Ground-state of ^{8}Li β decays with a half-life of 840 ms to an excited state of ^{8}Be which immediately breaks up into two α particles emitted in opposite directions. Such events should be easily identified in the OTPC. Surprisingly, only few events of this kind were observed. Instead, several events with a ^{8}He ion with single, diffused tracks was recorded. Closer analysis of these events showed that the width of tracks registered by the camera was significantly larger than the widths of tracks of ^{7}Li recoils from β-delayed neutron decay of ^{8}He. Moreover, the decay-time distribution of these events showed the grow-in and decay characteristics expected for the $^{8}\mathrm{He}\to{}^{8}\mathrm{Li}\to{}^{8}\mathrm{Be}$ decay sequence. These observation lead us to the conclusion that most of the decays of ^{8}Li occurred at the cathode where the ^{8}Li ions produced in the decay of ^{8}He have drifted. It was possible because: *(i)* the time needed for lithium ions to drift in helium gas under atmospheric pressure in the electric field of 250 V/m [14] is much shorter than the lifetime of ^{8}Li, *(ii)* due to the high ionization potential of helium atoms, lithium ions are not being neutralized on their way to the cathode. Since two α particles emitted after ^{8}Li decay are ejected in opposite directions, only one of them could enter the active volume of the detector and a single track was observed. The large width of the tracks is explained by the diffusion effects during long (30 cm) electron drift distance.

4. Summary and outlook

The feasibility of β-decay studies of ^{8}He by the use of the optical time projection chamber has been investigated. It was demonstrated, that β-delayed neutron emission events in the decay of ^{8}He can be observed by the registration of tracks of the recoiling ^{7}Li nuclei. Evidence for the neutron emission after β-decay of ^{8}He to a highly excited ^{8}Li state was obtained indicating that the reported decay scheme of ^{8}He is not complete. The OTPC detector offers new possibility to study β decay of ^{8}He into the $\alpha + t + n$ continuum. It was shown that the full kinematics of such events can be reconstructed. Information obtained with the use of the OTPC will allow us to clarify the mechanism of such a decay process.

Further studies of the decay of ^{8}He are planned. For this purpose a new version of the OTPC detector, covering larger (by 75%) fraction of fragments range distribution, is being built. To improve the efficiency of triggering of the data acquisition system, the new detector will be equipped with a veto counter, which will be used to reject events with ions which did not stop in the active volume of the OTPC chamber. Very high sensitivity of the OTPC detector will open the possibility to search for the, so far unidentified, β-delayed deuteron branch in the decay of ^{8}He. Such events will have a unique signature of two different charged particles (^{6}He and ^{2}H) emitted in opposite directions. The new detector will be also equipped with a γ-ray spectrometer which will be used to identify β-delayed particle emission to excited states of final nuclei.

REFERENCES

[1] P. Mueler *et al., Phys. Rev. Lett.* **99**, 252501 (2007).

[2] V.L. Ryjkov *et al., Phys. Rev. Lett.* **101**, 012501 (2008).

[3] T. Björnstad *et al., Nucl. Phys.* **A366**, 461 (1981).

[4] M.J.G. Borge *et al., Nucl. Phys.* **A460**, 373 (1986).

[5] M.J.G. Borge *et al., Nucl. Phys.* **A560**, 664 (1993).

[6] L.V. Grigorenko *et al., Nucl. Phys.* **A607**, 277 (1996).

[7] M.V. Zukhov *et al., Phys. Rev.* **C52**, 2461 (1995).

[8] M. Ćwiok *et al., IEEE Trans. Nucl. Sci.* **52**, 2895 (2005).

[9] K. Miernik *et al., Nucl. Instrum. Methods* **A581**, 194 (2007).

[10] K. Miernik *et al., Phys. Rev. Lett.* **99**, 192501 (2007).

[11] A.M. Rodin *et al., Nucl. Instrum. Methods* **B204**, 114 (2003).

[12] F. Sauli, *Nucl. Instrum. Methods* **A580**, 971 (2007).

[13] *The Stopping and Range of Ions in Matter (SRIM)*, `http://www.srim.org`

[14] T.H. Lovaas *et al., J. Phys.* **D20**, 1465 (1987).